

Preparation of the charge radii measurements of $^{8,9,11}\text{Li}$

W.Nörtershäuser, A. Dax, H. Wang, R. Kirchner, H.-J. Kluge, T. Kühl
GSI Darmstadt, Germany

I. Tannihata, M. Wakasugi
RIKEN, Saitama, Japan

C. Zimmermann
University of Tübingen, Germany

INTRODUCTION

The investigation of the so-called “halo nuclei”, *e.g.*, ^{11}Li , ^6He has become a hot topic in nuclear physics since the discovery by Tannihata *et al.* [1]. However, the correlation between proton and neutron distributions in these exotic nuclei is still an open question, since nuclear collision studies are mainly sensitive to the matter distributions and do not allow a model-independent determination of charge radii. On the other hand, on-line laser spectroscopic measurements of hyperfine structure and isotope shifts have long been used to investigate charge radii of stable and unstable isotopes [2]. Combined with recent progress in the atomic theory of lithium [3], such a measurement will allow a model-independent determination of the charge radius of $^{8,9,11}\text{Li}$. Therefore we prepare a precise measurement of isotope shifts for stable and short-lived isotopes of lithium at GSI in Darmstadt (Germany). Due to the low production rates of these exotic atoms ($\sim 10^4/\text{s}$ for ^{11}Li) a very sensitive technique must be developed that still allows an accurate determination of the differences in transition energies (relative accuracy $\sim 10^{-5}$). Resonance Ionization Spectroscopy (RIS) with cw-lasers has been used for the efficient detection of short-lived isotopes [4, 5] for many years and was found to be the most promising technique for our purpose. Results of test experiments in order to find the best excitation and ionization scheme were presented previously, together with a determination of the release efficiency for an on-line source of thermal lithium atoms [6]. In this report, we will give a short summary of the experimental approach and then focus on recent progress in the preparation of the laser-stabilization system and the characterization of the quadrupole mass spectrometer that will be used to detect the ions created by the laser resonance ionization process.

THEORY

The isotope shift (IS) in an optical transition can be divided into two parts: the mass shift (MS), caused by the difference in nuclear mass between the isotopes, and the field shift (FS), which has its origin in the change of the distribution of electrical charge inside the finite sized nucleus. The FS is directly related to the difference in the root-mean-square (rms) charge radius between two isotopes having masses A and A' :

$$\Delta E_{\text{FS}} = -\frac{2p}{3} Ze^2 |\psi(0)|^2 d\langle r^2 \rangle^{AA'}$$

Table 1. Calculated mass shifts in the $2^2S - 2^2P$ transition of lithium [3]. All values in MHz.

$^7\text{Li} - ^6\text{Li}$	$^8\text{Li} - ^6\text{Li}$	$^9\text{Li} - ^6\text{Li}$	$^{11}\text{Li} - ^6\text{Li}$
11453.07 (6)	20088.23 (10)	26785.18 (13)	36555.34 (21)

where $\Delta|\rho(0)|^2$ is the change of electron charge density at the nucleus between lower and upper state of the optical transition. A determination of the field shift can thus provide accurate values for the rms charge radius. However, the mass- and field shift contributions to the isotope shift cannot be separated easily, therefore additional information from muonic atoms and electron scattering is usually combined with optical isotope shift data to extract charge radii [7]. If it is possible, however, to calculate the mass shift in a transition to a sufficiently high accuracy, the field shift can be directly extracted without any additional information. But mass shift evaluations are difficult since electron-electron correlations must be included and many-body problems are hard to attack. It has nevertheless been used to determine rms charge radii for ^3He and ^6Li from ^3He - ^4He and $^6\text{Li}^+ - ^7\text{Li}^+$ isotope shift measurements [8].

Recent advances in high-precision variational calculations for lithium and lithiumlike ions using multiple basis sets in Hylleraas coordinates [9], allowed mass-shift calculations for the $2S-3S$ and $2S-2P$ transitions in Li with an accuracy of approximately 200 kHz [3]. Yan and Drake provided a formula for the nuclear charge radius of any Li isotopes as a function of the measured isotope shift between the isotope ^ALi and ^6Li :

$$R_{\text{rms}}^2(^A\text{Li}) = R_{\text{rms}}^2(^6\text{Li}) + \frac{E_{\text{meas}}^A - E_0^A}{C}$$

where E_{meas}^A is the measured isotope shift and E_0^A contains all calculated contributions to the isotope shift except for the nuclear size contribution. The calculated mass shifts E_0^A for all lithium isotopes are listed in Table 1 and the constant C for the $2s-3s$ transition was calculated to be $C = -1.5661 \text{ MHz/fm}^2$.

EXPERIMENTAL

The lithium isotopes of interest have lifetimes of 838 (6) ms (^8Li), 178.3 (4) ms (^9Li), and 8.59 (14) ms (^{11}Li), respectively, thus IS measurements can only be performed on-line. It is planned to produce $^{8,9}\text{Li}$ in a $^{12}\text{C} (^{12}\text{C}, X) ^{8,9}\text{Li}$ reaction at the GSI UNILAC accelerator and ^{11}Li at ISOLDE/CERN, where 1 GeV protons induce spallation and fragmentation inside a tantalum target. In both cases the Li ions produced are released from the hot target, accelerated to 60 keV and mass separated in a sector magnet. Ion yields of approximately $10^5/\text{s}$ ($^{8,9}\text{Li}$, GSI) and $10^4/\text{s}$ (^{11}Li , CERN) are available. Ions are implanted into a graphite catcher foil ($\sim 80 \mu\text{g}/\text{mm}^2$), where they recombine with electrons. The catcher foil is heated by a CO_2 laser beam to release the Li atoms with thermal velocities. Laser beams for resonance ionization are located close to the graphite surface to ensure a good overlap with the released atomic ensemble.

The excitation scheme for resonance ionization is shown in Fig. 1. After excitation to the $3S$ state in a two-photon transition, the atom undergoes spontaneous emission into the $2P$ state and is subsequently ionized through the $3D$ levels. The double-resonance four-photon ionization pathway has the following advantages:

- the $2S$ - $3S$ two-photon excitation provides efficient excitation independent of the Doppler shift.
- the ionization step is decoupled from the $2S$ - $3S$ transition, where high accuracy is needed, and the ionization step – ionization directly out of the $3S$ state would cause AC Stark shift and broadening and thus reduce accuracy.
- resonance enhancement for the ionization due to the intermediate $3D$ states, the $2P$ - $3D$ transition is the strongest transition in lithium and can easily be saturated, thus, providing high efficiency for the ionization.

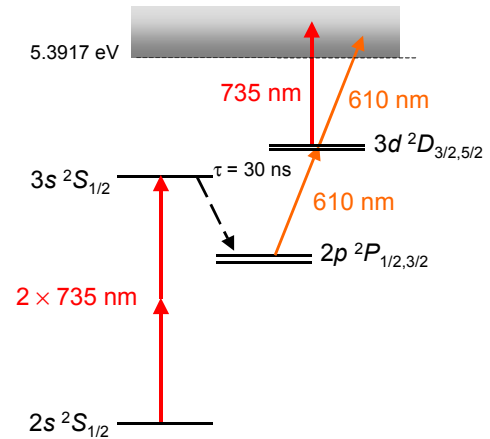


Figure 1. Excitation scheme for the resonance ionization of lithium

This ionization scheme was tested previously [6] and narrow lines with a FWHM of ~ 7 MHz were observed. Resonance ionization with single-ion detection was compared to fluorescence detection and was found to be ~ 20 times more efficient and to provide a higher signal to noise ratio even at moderate laser powers for the ionization step.

In Fig. 2 the experimental setup for the laser system (left) and resonance ionization mass spectrometry (right) is shown. The atoms released from the graphite catcher transverse the

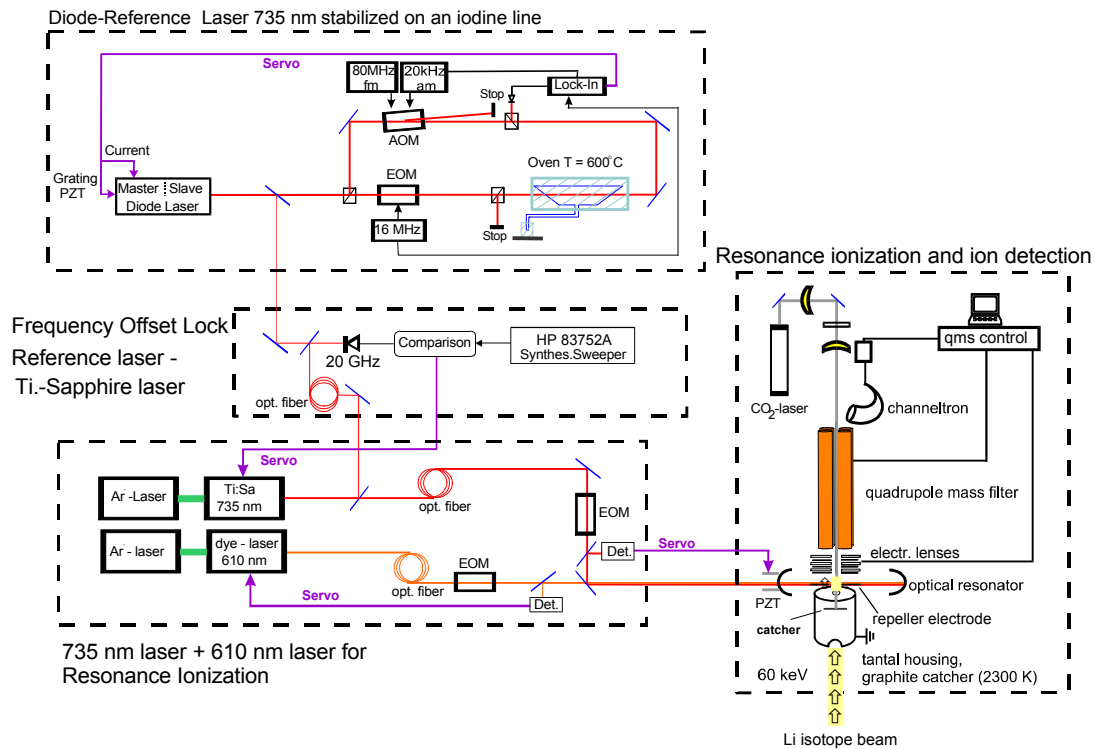


Figure 2. Experimental setup for the resonance ionization of lithium

laser beams and the laser-ionized particles are collected with the ion optics of a commercial quadrupole mass spectrometer, mass analyzed and detected with a conversion dynode electron multiplier (CDEM).

Resonant laser radiation is provided by a titanium-sapphire laser (Ti:Sa) (735 nm) and a dye laser (610 nm), which are both pumped by argon-ion lasers. To obtain intensities that are sufficient to saturate the two-photon resonance transition and to provide high ionization efficiency, an optical resonator is mounted into the vacuum system around the interaction region. The cavity must provide resonance enhancement for both laser beams at the same time. Thus, the cavity length is locked to the frequency of the Ti:Sa laser, while the dye laser frequency, which is less critical due to strong saturation broadening in the $2P-3D$ transition, is locked to the optical resonator.

Accurate frequency tuning and stabilization is obtained by frequency-offset-locking of the Ti:Sa to a master-slave diode-laser system, which is locked to an molecular-iodine transition to provide a reliable frequency reference point for consecutive measurements. To realize this frequency-offset locking, the iodine transition frequency must be close to half the resonance frequencies for all lithium isotopes of interest. The difference should be less than ~ 20 GHz in order to allow counting of the beat signal between the diode laser and the Ti:Sa beam by means of a standard radiofrequency counter. A hot-band transition at 13603.22 cm^{-1} fulfills this criteria, but the hyperfine spectrum and saturation intensities of this line have not been investigated previously.

RESULTS

Due to the low production rates for the short-lived ^{11}Li isotope an overall detection efficiency of $\sim 10^{-4}$ is required. The overall efficiency can be divided into the following parts: ion-to-atom-conversion efficiency of the graphite catcher, geometrical overlap between the atomic and laser beams, resonance ionization efficiency, transmission through the QMS and detection efficiency of the CDEM. The estimated or measured efficiencies for the different processes are listed in Tab. 2. The conversion efficiency in the graphite catcher as a function of temperature has been measured in previous experiments [6], and the geometrical overlap was calculated assuming a cosine-square distribution for the atomic beam and a 0.5 mm diameter laser beam spot in a distance of 1.5 mm. The ionization efficiency was estimated to be the product of an excitation efficiency to the $3S$ state of 20% (calculated on a basis of perturbation theory and verified experimentally), ionization efficiency of 3%, and a signal reduction of 65% due to the hyperfine splitting of the ground- and excited state. The product of the given efficiencies is slightly larger than 10^{-4} and should thus be sufficient to obtain an on-resonance count rate of

~ 1 Hz. The dark count rate of the CDEM was measured to be ~ 15 mHz and is thus considerably smaller than the expected signal rate.

The QMS works as an additional mass filter for background suppression of ions that are either created in the ionization region by processes other than resonance ionization or have enough energy to

Table 2. Expected efficiencies for processes involved in the ^{11}Li isotope shift measurement

release efficiency of the catcher	20 %
overlap with laser beams	20 %
excitation and ionization efficiency	0.5 %
quadrupole mass filter transmission	90 %
CDEM detector efficiency	80 %
overall detection efficiency	$\sim 10^{-4}$

penetrate into the ionization region. Peak shapes for the stable lithium isotopes have been recorded using a surface ionization ion source and are shown in Fig. 3 on a logarithmic scale. Due to the nearly flat-topped peaks, the transmission through the QMS is almost independent on the exact mass setting within a range of ~ 0.4 amu, but to the higher-mass side the signal drops sharply by more than 7 orders of magnitude. On the rising side the profiles are not as steep and exhibit a dip, which is caused by non-linear resonances [10] and leads to a kind of precursor peak. However, 0.5 amu below the mass of interest the signal intensity has decreased by a factor of $\sim 10^7$ and background contributions to the lithium signal should be small.

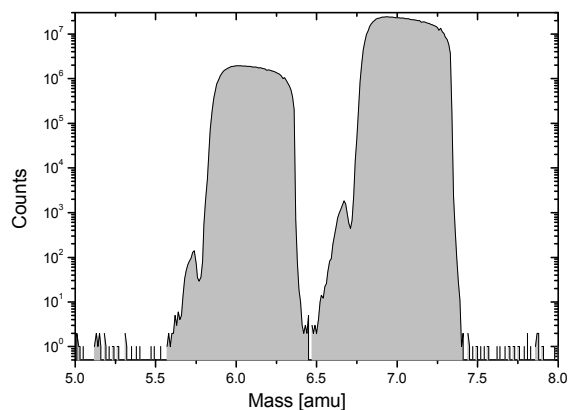


Figure 3. QMS mass spectrum of $^{6,7}\text{Li}$ ions produced by surface ionization

To obtain the isotope shift values with the required accuracy, an appropriate frequency reference point must be chosen for the frequency-offset locking of the resonance lasers to provide a relocking accuracy of better than a few 10 kHz. We performed FM-saturation spectroscopy on the iodine transition at 13603.22 cm^{-1} to test whether it could be used to obtain a saturation spectroscopy signal appropriate for laser-locking within the required accuracy. The experimental setup was similar to that shown in the rectangle on Fig. 2, marked as “Diode reference laser 735 nm” with the main difference that we used a Ti:Sa laser to obtain the saturation signal. The iodine cell was heated to $\sim 600^\circ\text{C}$ to provide sufficient population of the lower level of the hot-band transition. A saturation signal recorded with laser powers of 20 mW in the pump and 1 mW in the probe beam ($\varnothing 1\text{ mm}$, FWHM) is shown in Fig. 4. Three groups of unresolved and three single hyperfine lines were observed. The strongest isolated line (a_1) is well separated from all others and will be used for locking the diode laser. Signal-to-noise ratios of about 600 were achieved for this line and it shows a peak-to-peak distance of $\sim 10\text{ MHz}$, thus an accuracy of about 20 kHz for locking to the reference point can be expected.

The signal intensity of the chosen reference line was measured as a function of laser power in the pump beam. Saturation was clearly observed and a saturation intensity of 20 mW/mm^2 has been calculated. Such intensities should be available with the diode-laser master-slave system, which will be used as the reference laser for frequency offset locking.

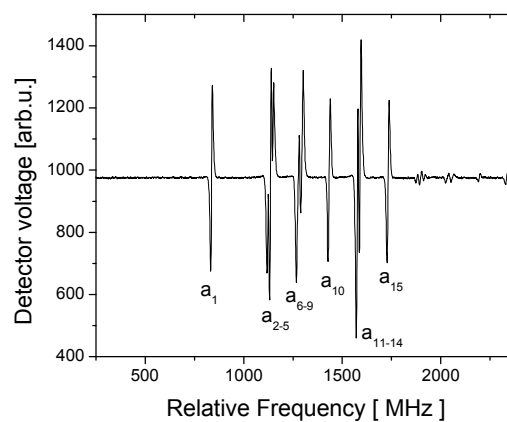


Figure 4. Hyperfine spectrum of the iodine $\text{B}0_{\text{u}}^+ \rightarrow \text{X}1\Sigma_{\text{g}}^+\text{R}(114)2-11$ transition at 600°C .

SUMMARY AND OUTLOOK

The experimental setup for isotope shift measurements of $^{8,9,11}\text{Li}$ is in progress. The vacuum chamber has been assembled and the QMS was characterized in terms of mass peak shape and detector dark count rate. Saturation spectroscopy of the hot-band iodine transition chosen as a frequency reference point was performed and its suitability for frequency locking of the reference laser was demonstrated. After set-up of the enhancement cavity, which is underway, and all necessary frequency-locking electronics, we will first test the whole setup in off-line measurements with the stable isotopes $^{6,7}\text{Li}$. Afterwards $^{8,9}\text{Li}$ measurements are planned at GSI, before transporting the whole setup to CERN to finally perform the measurements on ^{11}Li .

ACKNOWLEDGMENT

This work is supported by BMBF contract No. 06TU886/TP3

REFERENCES

1. Tanihata, I., et al., *Measurements of interaction cross sections and nuclear radii in the light p-shell region*. Physical Review Letters, 1985. **55**: p. 2676-2679.
2. Otten, E.W., *Nuclear radii and moments of unstable isotopes*, in *Treatise on heavy-ion science*, D.A. Bromley, Editor. 1989. p. 517-638.
3. Yan, Z.-C. and G.W.F. Drake, *Lithium isotope shifts as a measure of nuclear size*. Physical Review A, 2000. **61**: p. 022504.
4. Wendt, K., et al., *Recent developments in and applications of resonance ionization mass spectrometry*. Fresenius Journal of Analytical Chemistry, 1999. **364**: p. 471-477.
5. Bushaw, B.A., *High-resolution laser-induced ionization spectroscopy*. Prog. Analyt. Spectrosc., 1989. **12**: p. 247-276.
6. Schmitt, F., et al., *Towards the determination of the charge radius of ^{11}Li by laser spectroscopy*. Hyperfine Interactions, 2000. **127**: p. 111-115.
7. Fricke, G., et al., *Nuclear ground state charge radii from electromagnetic interactions*. Atomic Data Nuclear Data Tables, 1995. **60**: p. 177-285.
8. Riis, E., et al., *Lamb shifts and hyperfine structure in $^6\text{Li}^+$ and $^7\text{Li}^+$: Theory and experiment*. Physical Review A, 1994. **49**: p. 207-220.
9. Drake, G.W.F. and Z.-C. Yan, *Energies and relativistic corrections for the Rydberg states of helium: Variational results and asymptotic analysis*. Physical Review A, 1992. **46**: p. 2378-2409.
10. Blaum, K., et al., *Peak shape for a quadrupole mass spectrometer: comparison of computer simulation and experiment*. International Journal of Mass Spectrometry, 2000. **202**: p. 81-89.